

Gabrielle L. Clark-Patterson

Department of Biomedical Engineering,
Tulane University,
6823 St Charles Ave.,
New Orleans, LA 70118
e-mail: gclark2@tulane.edu

Jeffrey A. McGuire

Department of Biomedical Engineering and
Mechanics,
Virginia Tech,
330 A Kelly Hall,
325 Stanger Street,
Blacksburg, VA 24061
e-mail: jeffmcg8@vt.edu

Laurephile Desrosiers

Department of Female Pelvic Medicine &
Reconstructive Surgery,
University of Queensland Ochsner Clinical
School,
1514 Jefferson Highway,
New Orleans, LA 70121
e-mail: laurephile.desrosiers@ochsner.org

Leise R. Knoepp

Department of Female Pelvic Medicine &
Reconstructive Surgery,
University of Queensland Ochsner Clinical
School,
1514 Jefferson Highway,
New Orleans, LA 70121
e-mail: lknoepp@ochsner.org

Raffaella De Vita

Department of Biomedical Engineering and
Mechanics,
Virginia Tech,
330 A Kelly Hall,
325 Stanger Street,
Blacksburg, VA 24061
e-mail: devita@vt.edu

Kristin S. Miller¹

Department of Biomedical Engineering,
Tulane University,
6823 St Charles Ave.,
New Orleans, LA 70118
e-mail: kmille11@tulane.edu

Investigation of Murine Vaginal Creep Response to Altered Mechanical Loads

The vagina is a viscoelastic fibromuscular organ that provides support to the pelvic organs. The viscoelastic properties of the vagina are understudied but may be critical for pelvic stability. Most studies evaluate vaginal viscoelasticity under a single uniaxial load; however, the vagina is subjected to dynamic multiaxial loading in the body. It is unknown how varied multiaxial loading conditions affect vaginal viscoelastic behavior and which microstructural processes dictate the viscoelastic response. Therefore, the objective was to develop methods using extension-inflation protocols to quantify vaginal viscoelastic creep under various circumferential and axial loads. Then, the protocol was applied to quantify vaginal creep and collagen microstructure in the fibulin-5 wildtype and haploinsufficient vaginas. To evaluate pressure-dependent creep, the fibulin-5 wildtype and haploinsufficient vaginas ($n=7/genotype$) were subjected to various constant pressures at the physiologic length for 100 s. For axial length-dependent creep, the vaginas ($n=7/genotype$) were extended to various fixed axial lengths then subjected to the mean in vivo pressure for 100 s. Second-harmonic generation imaging was performed to quantify collagen fiber organization and undulation ($n=3/genotype$). Increased pressure significantly increased creep strain in the wildtype, but not the haploinsufficient vagina. The axial length did not significantly affect the creep rate or strain in both genotypes. Collagen undulation varied through the depth of the subepithelium but not between genotypes. These findings suggest that the creep response to loading may vary with biological processes and pathologies, therefore, evaluating vaginal creep under various circumferential loads may be important to understand vaginal function. [DOI: 10.1115/1.4052365]

1 Introduction

The vagina is a viscoelastic fibromuscular organ that connects the uterus and cervix to the outside of the body [1–9]. It plays a role in intercourse and childbirth and provides support to the pelvic organs (e.g., uterus, bladder, rectum). Failure in pelvic organ support leads to the descent of one or more pelvic organs into the vaginal canal known as pelvic organ prolapse (POP). This decreases the quality of life and results in 11–13% of women requiring surgical intervention to restore anatomy and alleviate symptoms [10,11]. The underlying processes that contribute to

POP are not fully understood, however, vaginal birth [12], aging [12], body mass index [13,14], and excessing heavy lifting [15] are established risk factors. Prior studies suggest that the viscoelastic properties of the pelvic structures are critical for vaginal birth to facilitate delivery minimizing maternal injury and subsequent pelvic floor disorders [16–21]. Further, the pelvic floor must withstand repetitive loading due to everyday activities (i.e., walking, sitting, running, coughing, etc.) [22–24]. Hence, a fundamental understanding of vaginal viscoelastic behavior in a dynamic mechanical environment is critical for elucidating its role in pelvic stability. Further, this may help us better understand structural processes as a result of an injury that may lead to POP over time.

The vagina deforms over time under a constant load which is known as creep [4]. Various soft tissues demonstrate that the rate of creep and degree of deformation depends on the load applied

¹Corresponding author.

Manuscript received March 1, 2021; final manuscript received August 27, 2021; published online October 11, 2021. Assoc. Editor: Sara Roccabianca.

[21,25–27]. The vagina is subjected to a dynamic and evolving multi-axial mechanical environment due to the fluctuation of intra-abdominal pressure with daily activities [22–24]. Currently, it is unknown how mechanical loading affects the creep behavior and what microstructural processes contribute to this behavior in the vagina. To date, most studies evaluate vaginal viscoelasticity under a single uniaxial load. However, there is a need for biomechanical tools evaluating vaginal creep while subjected to various multi-axial loading conditions.

Inflation protocols evaluated creep of the colon [28] and blood vessels [27,29] under various loading conditions by pressure. Furthermore, free and fixed axial extension-inflation protocols recently quantified the elastic mechanical properties of the rodent vagina [30–34]. Extension-inflation protocols are advantageous, as they maintain intact organ geometry and extracellular matrix interactions. The intact geometry permits subjecting the tissue to a defined range of physiologically relevant pressures and axial extensions. Extension-inflation protocols may also be useful for evaluating vaginal creep with varied multi-axial loading conditions. Our objective was to develop methods using extension-inflation protocols to quantify vaginal creep under various circumferential and axial loads. It was hypothesized that vaginal creep strain and rate increase with increased pressure and axial length.

Prior studies suggest that collagen fiber uncrimping contributes to the viscoelastic creep response [26,35]. Further, that collagen fiber undulation may be dictated, in part, by physical constraints due to the elastic fibers within the extracellular matrix [31,36]. Toward this end, murine models with elastic fiber defects are tools to evaluate potential elastic-collagen fiber interactions and their subsequent effect on biomechanical properties [36,37]. Fibulin-5 is a protein critical for elastic fiber assembly and fibulin-5 deficient mice develop prolapse similar to the clinical presentation in humans [38,39]. However, 92% of the fibulin-5 deficient mice develop severe prolapse by 6 months of age [39]. Therefore, the fibulin-5 haploinsufficient (one copy of the gene) model was used as an initial step to extend the extension-inflation creep protocols independent of the prolapse state. Previous work demonstrated a significant increase in matrix metalloproteinase-9 (MMP9) enzymatic activity in the fibulin-5 haploinsufficient mice vaginal tissue compared to the wildtype [39]. Some studies also show that MMP9 has an affinity for elastin [40,41]. Based on previous findings, it was hypothesized that increased MMP9 activity may disrupt elastic fibers in the fibulin-5 haploinsufficient model with subsequent changes in collagen microstructure. Further, it was hypothesized that vaginal creep strain and rate are greater in the fibulin-5 haploinsufficient vagina compared to the wildtype control.

2 Methods

2.1 Sample Collection. The Institute Animal Care and Use Committee at Tulane University approved all procedures in this study. National, international, and institutional guidelines for the care and use of animals were followed. Female and male fibulin-5 (*Fbln5*) haploinsufficient mice on the mixed background (C57BL/6 × 129 SvEv) generated all female wildtype (*Fbln5*^{+/+}) and haploinsufficient (*Fbln5*^{+/-}) mice used in this study [42]. Real-time polymerase chain reaction confirmed the presence or absence of *Fbln5* (Transnetyx, Inc., Cordova, TN). All animals were housed under standard housing conditions in a 12-hour light/dark cycle at room temperature (20 °C) with free access to food and water. This study euthanized 54 ($n = 27/\text{genotype}$) 3–6 months of age female mice by carbon dioxide inhalation at estrus by visual assessment [43]. This age range corresponds to 20–30 human years which is past development but not affected by senescence thus representing the sexually mature adult group [44]. A pilot study in both genotypes ($n = 3/\text{age group}$) demonstrated that age did not significantly affect creep (3–4 versus 5–6 months). The female reproductive system was removed, and microscissors separated the vagina from

the cervicovaginal complex. The vaginal tissue was snap frozen in liquid nitrogen followed by storage at $-80\text{ }^{\circ}\text{C}$ (-353 K) until mechanical testing or imaging [7,45]. On the day of testing or imaging, the samples were thawed at room temperature (20 °C; 293 K).

2.2 Pressure Catheterization. A balloon catheter measured intravaginal pressure on a separate cohort of 3–6 months of age female *Fbln5*^{+/+} and *Fbln5*^{+/-} mice ($n = 6/\text{genotype}$) at estrus to recapitulate the mechanical loads in vitro during mechanical testing [32,46–49]. A custom polyvinyl chloride 3 mm-diameter balloon was secured onto a 1.25 mm-diameter aluminum tube creating the balloon catheter. A three-way stopcock connected the balloon catheter to the front port of the pressure transducer (-50 to $+300$ mmHg; Product number MLT0699; ADInstruments, Colorado Springs, CO). Further, a 3-mL syringe filled with water was connected to back port of the pressure transducer [32]. The pressure transducer was connected to a laptop and system software (PowerLab and LabChart8, ADInstruments, Colorado Springs, CO) [32]. The 3-mL syringe filled the aluminum tube and balloon with water distending the balloon to 3 mm and the pressure transducer measured the baseline pressure [32]. On anesthetized mice (4% isoflurane in 100% oxygen) the balloon was inserted into the vaginal canal. The pressure transducer measured the current pressure and the change between the current and baseline pressure quantified the in vivo pressure [48]. All animals underwent balloon catheterization three times to minimize user variability and to quantify the average intravaginal pressure readings [32]. The mean in vivo vaginal pressure was 7.4 ± 0.8 mmHg and 5.4 ± 0.5 mmHg for the wildtype and haploinsufficient mice, respectively (mean \pm SEM; see Fig. 1 available in the Supplemental Materials on the ASME Digital Collection). Unpaired t-test did not detect statistically significant differences between genotype in in vivo vaginal pressure measurements. These pressure values were used to recapitulate in vivo loading in the in vitro creep experiments about an estimated physiologic range.

2.3 Experimental Set-Up. An extension-inflation device (Biodynamic 5170 System; TA Instruments Electroforce, New Castle, DE) evaluated the creep response of the murine vagina.

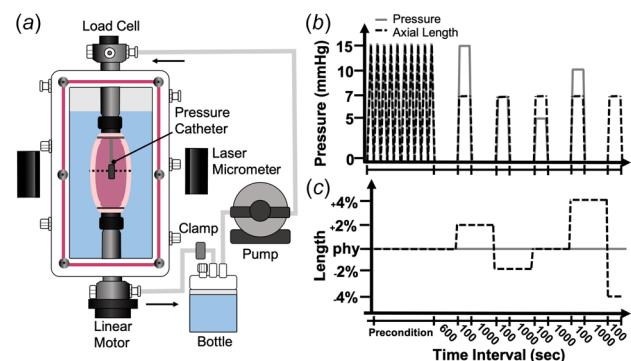


Fig. 1 Schematic of extension-inflation device (a). The laser micrometer projected onto the middle-third anterior vaginal wall measured axial load and the linear motor axially extended the vagina. A clamp controlled the pump drive. The pump and pressure catheter controlled and measured pressure in the vaginal lumen. The arrows show the direction of flow. Prior to all tests the vagina underwent 10 cycles of preconditioning (a) at the physiologic length (phy; b), followed by 600 s of equilibration. Four constant randomized pressures (5, 7, 10, and 15 mmHg) evaluated the pressure-dependent creep response (grey line) at the physiologic length. Five randomized fixed axial lengths ($\pm 2\%$, $\pm 4\%$, physiologic length) evaluated the axial length-dependent creep response (black dashed lines) under the mean in vivo pressures.

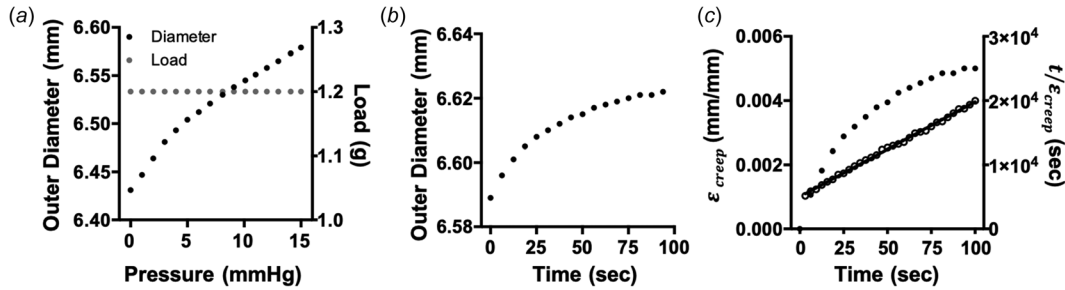


Fig. 2 Representative graph of outer diameter (black) and load (grey) response to increasing pressure (a). At the experimental physiologic length load held constant under increasing pressure. Representative outer diameter curve over 100 s of creep under a constant 15 mmHg (b). Representative strain (filled; left y-axis) versus time curve for 100 s of creep (c). Peleg's equation linearly transformed the strain versus time curve (open; right y-axis) [63]. A linear regression determined the slope and intercept of the linear line (black line). Outer diameter and creep strain are reported every 6 s for visualization. In this figure, the representative linear transformed curve is reported every 3 s demonstrating data analysis.

Inflation methods investigated the viscoelastic properties of various soft tissues [27–29,50] and permitted maintenance of intact organ geometry and extracellular matrix interactions to subject the tissue to physiologically relevant pressures. Before mechanical testing, the tissue was thawed at room temperature for 10 min. Room temperature Hanks balanced salt solution kept the tissue hydrated throughout the biomechanical test [7,45]. Two 6–0 sutures secured the vagina onto custom 3.75-mm cannulas with the proximal region on the top cannula and the distal on the bottom cannula (Fig. 1(a)). A pressure catheter placed in the lumen of the vagina (3.5 F Mikro-Cath Part # 825-0101, 500 mmHg/67 kPa maximum pressure, accuracy ± 0.5 mmHg/0.07 kPa, Millar, Houston, TX) in a feedback loop with a pump (I-Drive model 76003; Micropump Inc., Vancouver, WA) controlled and measured pressure. Tubing (OD High-Pressure Silicone Rubber Tubing, Part # 5157K43, McMaster-Carr, Robbinsville, NJ) attached a 250-mL bottle filled with Hanks balanced salt solution to the pump, then from the pump to the top port of the cannula. Another tube attached the bottom port of the cannula back to the bottle creating a continuous closed flow loop. An adjustable clamp attached to the downstream tube controlled the pump drive.

A laser micrometer (Mitutoyo LSM-503S Laser Scan Micrometer with LSM-6200 Display, 2 μ m resolution, Mitutoyo Corporation, Kanagawa, Japan) optically tracked outer diameter at the mid-anterior vaginal wall. Before testing, the laser micrometer was calibrated according to the manufacture instructions to account for changes between the acrylic material and testing solution. A load cell (1000 g/9.8 N; 0.03 g/0.0003 N resolution) connected to the top cannula measured load and the linear motor (linear displacement ± 6.5 mm; 1 μ m resolution) attached to the bottom cannula axially extended the vagina. The WINTEST software (TA Instruments Electroforce, New Castle, DE) controlled the linear motor and pump pressure. After mounting the biochamber, the caps on the top ports were removed to eliminate pressure build-up within the system. The WINTEST software increased pressure to 5 mmHg (0.67 kPa), followed by adjusting the clamp (tightened or loosened) to operate the pump drive at 5%. Rates larger than this resulted in fast-turbulent flow interfering with the outer diameter measurement.

The linear motor axially extended the vagina from the unloaded length to the experimental physiologic length [29–31,33,51–53]. Explanting the vagina and removing the natural tethering, such as the paravaginal fascia, resulted in the vagina retracting or shortening in length [30–33]. Measuring the in vivo to ex vivo change in vaginal axial length between stain lines placed during dissection initially estimated retraction of the vagina [30,33,52]. The load cell further evaluated the physiologic length experimentally under the assumption that the load is constant over a range of increasing pressures to preserve energy as previously described (Fig. 2(a)) [29,53]. During the creep test, a 3-mmHg (0.40 kPa) tare pressure

prevented the vagina from collapsing to permit consistent and repeatable biomechanical testing [30–33]. At the physiologic length, 10 cycles of pressurization from 0 to 15 mmHg (0–2.00 kPa) at 1.5 mmHg/s preconditioned the vagina to obtain a repeatable response in outer diameter measurements (Fig. 1(b)) [30–33]. After preconditioning the vagina equilibrated for 10 min at the physiologic length and no pressure [30–33].

2.4 Creep Testing. Two protocols assessed creep as a function of loading by pressure or axial extension in separate cohorts of mice. The first protocol assessed vaginal creep as a function of pressure in the *Fbln5*^{+/-} and littermate control *Fbln5*^{+/+} mice ($n = 7$ /genotype). After equilibration, at the physiologic length pressure increased to a target pressure of 5 mmHg (0.67 kPa), 7 mmHg (0.93 kPa), 10 mmHg (1.33 kPa), or 15 mmHg (2.00 kPa) at 1.5 mmHg/s (Fig. 1(b)). The rate of pressurization aimed to minimize the development of dynamic effects [28,50]. The pressure was held constant for 100 s [32]. Creep and recovery are time intensive presenting challenges in obtaining multiple data sets

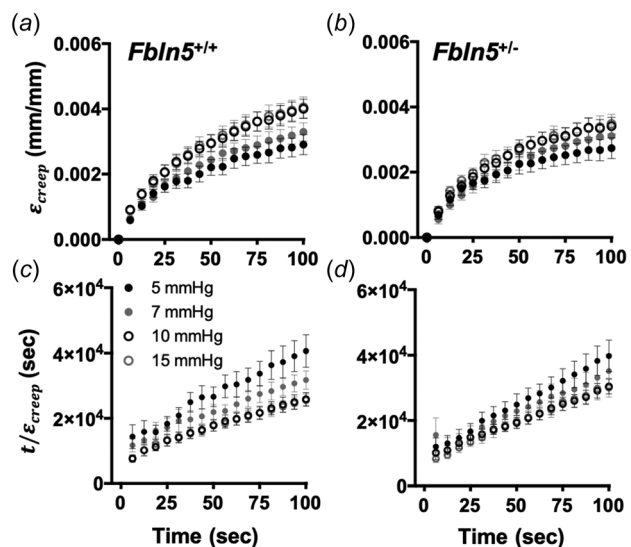


Fig. 3 Creep strain versus time curves for the *Fbln5*^{+/+} (a; $n = 7$) and *Fbln5*^{+/-} (b; $n = 7$) vaginas at 5 (black filled circle), 7 (grey filled circle), 10 (black open circle), and 15 (grey open circle) mmHg of constant pressure. The *Fbln5*^{+/+} creep strain curves for 10 and 15 mmHg shifted upward compared to 5 and 7 mmHg. Linear transformed curve using Peleg's equation for the *Fbln5*^{+/+} (c) and *Fbln5*^{+/-} (d) vaginas. Data is reported as mean \pm SEM.

Table 1 Peleg's constants, initial creep rate, and creep strain at 100 s for pressure-dependent creep test

	5 mmHg	7 mmHg	10 mmHg	15 mmHg
<i>Fbln5^{+/+}</i> (<i>n</i> = 7)				
k_1 ($\times 10^2$, sec)	118 \pm 20	115 \pm 26	79 \pm 13	80 \pm 15
k_2	298 \pm 42	209 \pm 26	188 \pm 16 ^a	182 \pm 19 ^a
R^2	0.94 \pm 0.02	0.90 \pm 0.05	0.97 \pm 0.01	0.95 \pm 0.03
Initial creep rate ($\times 10^{-4}$, sec ⁻¹)	0.95 \pm 0.11	1.09 \pm 0.17	1.45 \pm 0.20	1.44 \pm 0.17
Creep Strain ($\times 10^{-3}$, mm/mm)	2.91 \pm 0.31	3.30 \pm 0.28	4.01 \pm 0.30	4.05 \pm 0.32 ^a
<i>Fbln5^{+/-}</i> (<i>n</i> = 7)				
k_1 ($\times 10^2$, s)	101 \pm 24	111 \pm 17	90 \pm 18	71 \pm 10
k_2	302 \pm 46	236 \pm	211 \pm 18	240 \pm 26
R^2	0.96 \pm 0.01	0.89 \pm 0.04	0.98 \pm 0.01	0.95 \pm 0.01
Initial creep rate ($\times 10^{-4}$, sec ⁻¹)	1.37 \pm 0.28	1.06 \pm 0.17	1.38 \pm 0.25	1.57 \pm 0.56
Creep Strain ($\times 10^{-3}$, mm/mm)	2.78 \pm 0.30	3.11 \pm 0.35	3.32 \pm 0.30	3.49 \pm 0.30

^a*p* < 0.05 compared to 5 mmHg. Data is reported as mean \pm SEM.

within the same sample. In women, intravaginal pressure measurements constantly change with daily activities [22], therefore, a shorter time period may better represent the physiologic condition and permit multiple creep assessments within a single sample. Studies suggest that 100 s creep tests are advantageous in ligaments to compare viscoelastic properties within the same sample [54,55]. Therefore, this study used a 100 s creep test to permit investigating the creep response to various loading conditions on the same sample. Although this timeframe does not describe the entire creep behavior of the vagina, it will provide an initial quantification of the viscoelastic behavior supported by the greatest creep rate being observed within the first 60 s of the test (See Fig. 2 available in the Supplemental Materials on the ASME Digital Collection). After 100 s of creep, the pressure returned to 0 mmHg (not including tare) for 1000 s of recovery. This was 10 times longer than the duration of the creep test as previously recommended for recovery [56]. A pilot study demonstrated that three repeated 100 s creep tests with 1000 s for recovery did not significantly affect creep (See Fig. 3 and Table 1 available in the

Supplemental Materials), thus suggesting that the creep phenomenon in the vagina effectively recovered between 100 s creep test [57]. This protocol was repeated at the remaining, randomly allocated target pressures (5, 7, 10, or 15 mmHg). Random allocation was performed to minimize any artifacts that may be due to the order that the higher loads were applied [26].

The second protocol assessed creep as a function of axial length in the *Fbln5^{+/-}* and littermate control *Fbln5^{+/+}* mice (*n* = 7/genotype). After equilibration, the linear motor axially extended the vagina to the physiologic length, 4% above the physiologic length, 2% above the physiologic length, 4% below the physiologic length, or 2% below the physiologic length at 0.01 mm/s (Fig. 1(c)) [30–33]. The pump pressurized the vagina to the mean in vivo vaginal pressures of 7 mmHg (*Fbln5^{+/+}*) or 5 mmHg (*Fbln5^{+/-}*) at 1.5 mmHg/s and pressure held constant for 100 s. Pressure returned to 0 mmHg (not including tare) for 1000 s of recovery. This protocol was repeated at the remaining, randomly allocated axial lengths. The objective of this protocol was to assess creep as a function of axial length under a single pressure

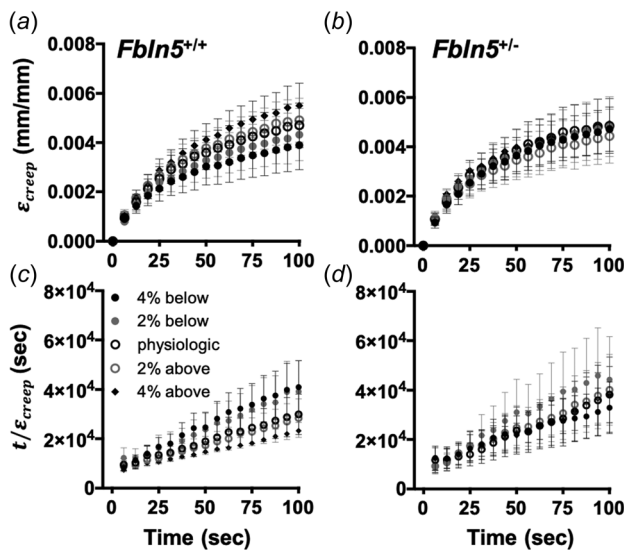


Fig. 4 Creep strain versus time curves for the *Fbln5^{+/+}* (a; *n* = 7) and *Fbln5^{+/-}* (b, *n* = 7) vaginas at 4% below (black filled circle), 2% below (grey filled circle), physiologic length (black open circle), 2% above (grey open circle), and 4% above (black filled diamond) the physiologic length. The *Fbln5^{+/+}* creep strain curve for 4% above the physiologic length shifted upward compared to 4% below the physiologic. Linear transformed curves using Peleg's equation for the *Fbln5^{+/+}* (c) and *Fbln5^{+/-}* (d) vaginas. Data is reported as mean \pm SEM.

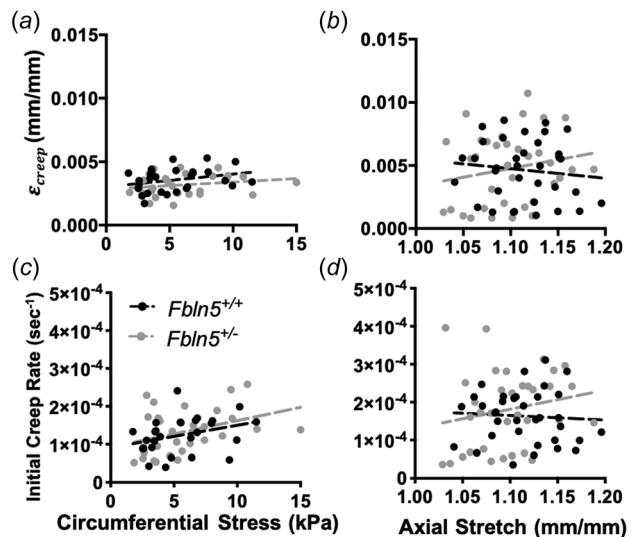


Fig. 5 Creep strain versus circumferential Cauchy stress from pressure-dependent creep test in the *Fbln5^{+/+}* (black) and *Fbln5^{+/-}* (grey) vaginas (a). The figure includes all data points from all pressure loading conditions. Creep strain versus axial stretch from axial length-dependent creep test (b). The figure includes all data points from all axial loading conditions. Initial creep rate versus circumferential stress from pressure-dependent creep test (c). Initial creep rate versus axial stretch from axial length-dependent creep test (d). Pearson's and Spearman's test did not detect significant correlations.

condition. While the physiologic length for each animal was identified, the pressure for each animal was not used because this would result in creep being dependent on pressure and not solely axial length. The mean in vivo pressure was selected as the single pressure for each genotype. The same pressure was not used for both genotypes because the purpose of this experiment was to assess changes in creep with axial length under the mean in vivo pressure condition using the balloon catheterization data. Further, the pressure-dependent studies provide information on how vaginal creep behavior responds under the same pressure conditions. For the pressure-dependent studies, the experimental physiologic length was constant with the same varied pressure (5, 7, 10, and 15 mmHg). For the length-dependent studies, the physiologic mean in vivo pressure was constant with varying axial length at the same degree ($\pm 2\%$, $\pm 4\%$, and physiologic length). During creep axial force decreased 1-4 mN and the axial force did not

fully recover (See Figs. 4 and 5 available in the [Supplemental Materials](#) on the ASME Digital Collection).

2.5 Ultrasound Imaging. In other biological soft tissues creep was evaluated with stress-controlled experiments [25,26,57]. This study used controlled static pressure to mimic the in vivo measured vaginal pressures then the mid-wall vaginal stress was calculated [27,28]. The laser micrometer could not measure the thickness of the vaginal wall during testing. Therefore, an ultrasound system was used after the test to assess vaginal wall thickness at each pressure used for the pressure-dependent creep test (5, 7, 10, 15 mmHg) [32,33]. After recovery from the last pressure-dependent creep test, B-mode ultrasound imaging with a 40 MHz transducer (Vevo2100; FUJIFILM VisualSonics, Toronto, Canada) measured vaginal wall thickness at the

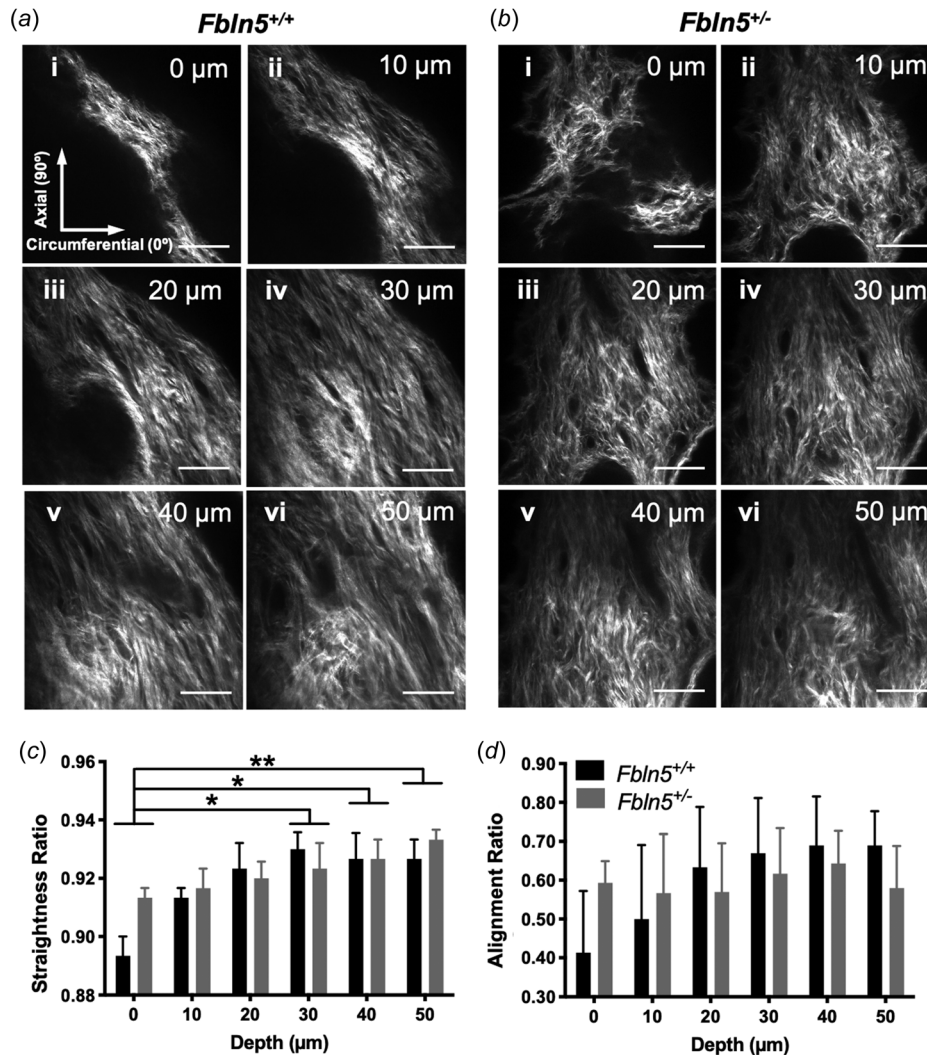


Fig. 6 Representative images of the collagen fiber network in the *Fbln5*^{+/+} (a) and *Fbln5*^{+/-} (b) vaginas. Images are displayed through the depth of the subepithelium at 0 (i), 10 (ii), 20 (iii), 30 (iv), 40 (v) and 50 (vi) μm. The depth of 0 μm denotes the start of the subepithelium from the epithelial layer. The straightness ratio is reported through the depth of the subepithelium in the *Fbln5*^{+/+} (black; $n = 3$) and *Fbln5*^{+/-} (grey; $n = 3$) vaginas (c). A two-way analysis of variance (ANOVA) for location and genotype demonstrated that location significantly affected the mean straightness ratio. Genotype did not significantly affect the mean straightness ratio and the statistical analysis did not detect significant interactions. Posthoc test for location differences (independent of genotype) demonstrated that the straightness ratio significantly increased at 30, 40, and 50 μm compared to 0 μm. The alignment ratio is reported through the depth of the subepithelium (d). Data is reported as mean \pm SEM. Statistical significance is reported as * $p < 0.05$ and ** $p < 0.01$. Scale = 50 μm.

physiologic length under 5, 7, 10, and 15 mmHg (See Fig. 6 available in the [Supplemental Materials](#) on the ASME Digital Collection). IMAGEJ quantified vaginal wall thickness (h) by drawing 25 lines across the wall [32,33,58]. A line drawn from the left to right lateral wall measured the outer diameter (d_o). This was performed 3 times on a single image then the measurements were averaged. A preliminary Bland Altman analysis ($n=3/\text{genotype}$) comparing the diameters between the ultrasound and laser micrometer (at 5, 7, 10, and 15 mmHg) demonstrated that measurements were in good agreement. This indicated that the ultrasound evaluated the same region as the laser micrometer during creep and that the thickness and outer diameter values can be used for the stress analysis. Volume and circumferential Cauchy stress (Eq. (1)) were calculated at 5, 7, 10, and 15 mmHg of pressure (P) using the ultrasound measured thickness and outer diameter [59]. The pressure did not significantly affect vaginal wall thickness and volume (See Fig. 6 available in the [Supplemental Materials](#)).

$$\sigma_\theta = \frac{P \left(\frac{d_o}{2} - h \right)}{h} \quad (1)$$

2.6 Creep Data Analysis. The outer diameters (d_o) measured by the laser micrometer during creep were normalized with reference to the outer diameter at 0 s (Figs. 2(b) and 2(c)) to quantify creep strain (Eq. (2)). Zero seconds ($t = 0$) denoted the start of the creep experiment when the target pressure was achieved during pressurization. This did not include the changes in diameter due to the elastic response (i.e., elastic strain) and was selected as the reference for this study in order to compare the accumulation of deformation across loading conditions. This was similar to subtracting the elastic strain from the creep response [60–62].

$$\epsilon_{\text{creep}} = \frac{d_o(t) - d_o(0)}{d_o(0)} \quad (2)$$

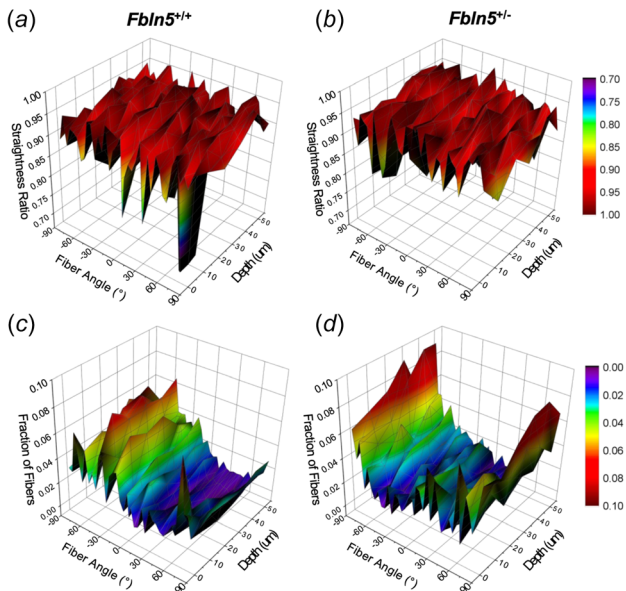


Fig. 7 Analysis of collagen fiber straightness ratio every 5 deg angled between -90 deg and 90 deg through the depth of the subepithelium in the $Fbln5^{+/+}$ (a; $n=3$) and $Fbln5^{+/-}$ (b; $n=3$) vaginas. A fiber angle of ± 90 deg represents the axial direction and a value of 0 deg represents the circumferential direction. The depth of $0 \mu\text{m}$ denotes the start of the subepithelium from the epithelial layer. Analysis of the fraction of fibers every 5 deg angled between -90 deg and 90 deg through the depth of the subepithelium in the $Fbln5^{+/+}$ (c; $n=3$) and $Fbln5^{+/-}$ (d; $n=3$) vaginas. The mean values are reported.

To compare the creep data, Peleg's equation transformed the non-linear strain versus time curve to a linear relationship by dividing time by strain (Eq. (3); Fig. 2(c)) [63]. This method recently described stress relaxation of the vagina [3] and previously evaluated creep in other applications such as food [63–65]. A linear regression determined Peleg's constants k_1 and k_2 (Eq. (3)). The reciprocal of constant k_2 represents the hypothetical asymptotic level for strain [63,65]. The reciprocal of k_1 describes the initial rate of creep.

$$t/\epsilon_{\text{creep}}(t) = k_1 + k_2 t \quad (3)$$

Analysis was performed every 3 s from 0 to 100 s. Data is reported every 6 s in order to easily visualize data across all loading conditions (Fig. 2(c)). The deformed axial length with respect to the unloaded axial length calculated the axial stretch ratio [59].

2.7 Second Harmonic Generation. Second harmonic generation (SHG) imaging was performed to examine the collagen organization within the vaginas of the $Fbln5^{+/-}$ and littermate control $Fbln5^{+/+}$ mice ($n=3/\text{genotype}$). Three vaginal tissue specimens from each group were collected and used for imaging. Before imaging, all tissue specimens were thawed in phosphate-buffered saline (pH 7.4, Dot Scientific, Burton, MI) at room temperature for 10 min. Tissue specimens were cut along the axial length of the vagina midway between the anterior and posterior walls, laid flat, and bonded onto a Petri dish with cyanoacrylate adhesive, exposing the inner squamous epithelial layer. The dish was filled with phosphate-buffered saline to maintain hydration throughout imaging. A Zeiss LSM 880 upright confocal multiphoton microscope (Zeiss, Thornwood, NY) with a motorized stage was used for backward-SHG imaging. A Ti:Sapphire laser (Ultra 1, Coherent, Santa Clara, CA) producing a linearly polarized beam with 140-fs duration pulses spectrally centered at 780 nm illuminated the specimens. The beam was reflected by a 690-nm short-pass dichroic mirror and focused onto the tissue specimens with a 40x, numerical aperture of 0.75, water-immersion microscope objective (W N-ACHROPLAN, Zeiss, Thornwood, NY). The average excitation power illuminating the tissue specimen was kept to less than 30 mW, as measured by a power meter (1936-C, Newport Corp., Irvine, CA), to prevent any damage to the tissue specimens. The beam was scanned across the tissue specimens by a galvanometric x-y scanner. The backscattered SHG signals from the tissue specimens traveled back through the same objective and were collected by a detector (BiG.2 module, Zeiss, Thornwood, NY) after passing through a 390-nm bandpass filter (Semrock FF01-390/18-25, IDEX Health & Science, LLC, Rochester, NY). The 390 nm bandpass filter separates the SHG signal from any generated autofluorescence. The two-dimensional images captured a region of $212.55 \times 212.55 \mu\text{m}^2$.

Six images were acquired from each tissue specimen within the $Fbln5^{+/+}$ and $Fbln5^{+/-}$ groups for a total of 36 images. Images were obtained from the mid-anterior wall at six different positions through the thickness (z -axis) of each vagina separated by $10\text{-}\mu\text{m}$ increments. The first z -axis position was selected by slowly increasing the depth of the focus plane with the focus drive attached to the microscope from the inner squamous epithelium until reaching the first collagen fiber signals. This position was marked as the reference z -axis position ($z = 0 \mu\text{m}$) and an image was acquired. The depth was increased by $10 \mu\text{m}$ ($z = 10 \mu\text{m}$), an image was acquired, and this process was repeated until the sixth image at a depth of $50 \mu\text{m}$ ($z = 50 \mu\text{m}$) from the reference position was acquired. The penetration depth was determined from a preliminary histological analysis with Masson's trichrome ($n=3/\text{genotype}$) where the subepithelium was 15% of the total vaginal wall thickness. Further, a noncontact laser micrometer (Keyence LK-G82, $0.2 \mu\text{m}$ resolution, Keyence Corporation, Itasca, IL) measured the thickness of the mid-anterior vaginal wall cut along the axial length ($n=2/\text{genotype}$) with an average thickness of

Table 2 Peleg's constants, initial creep rate, and creep strain at 100 s for axial length-dependent creep test

	4% below	2% below	physiologic	2% above	4% above
<i>Fbln5^{+/+}</i> (<i>n</i> = 7)					
<i>k</i> ₁ (×10 ² , sec)	78 ± 16	89 ± 32	82 ± 18	73 ± 12	68 ± 13
<i>k</i> ₂	345 ± 108	305 ± 109	221 ± 68	208 ± 68	158 ± 37
<i>R</i> ²	0.94 ± 0.02	0.95 ± 0.02	0.96 ± 0.02	0.94 ± 0.03	0.97 ± 0.01
Initial creep rate (×10 ⁻⁴ , sec ⁻¹)	1.60 ± 0.27	1.56 ± 0.22	1.59 ± 0.30	1.66 ± 0.31	1.76 ± 0.28
Creep strain (×10 ⁻³ , mm/mm)	3.90 ± 0.99	4.32 ± 0.11	4.70 ± 0.91	4.91 ± 0.90	5.38 ± 0.85
<i>Fbln5^{+/-}</i> (<i>n</i> = 7)					
<i>k</i> ₁ (×10 ² , sec)	113 ± 39	78 ± 22	81 ± 27	83 ± 26	90 ± 25
<i>k</i> ₂	216 ± 66	403 ± 179	286 ± 117	311 ± 122	284 ± 75
<i>R</i> ²	0.92 ± 0.03	0.94 ± 0.03	0.97 ± 0.01	0.95 ± 0.03	0.94 ± 0.03
Initial creep rate (×10 ⁻⁴ , sec ⁻¹)	1.65 ± 0.46	1.86 ± 0.35	1.98 ± 0.44	1.91 ± 0.34	1.63 ± 0.36
Creep strain (×10 ⁻³ , mm/mm)	4.83 ± 0.84	4.82 ± 1.22	4.85 ± 1.12	4.58 ± 1.02	4.91 ± 1.37

Data is reported as mean ± SEM.

325 ± 82 μm (mean ± SEM). Therefore, the subepithelium thickness was estimated to be 49 ± 12 μm (mean ± SEM). Unlike other tissues such as the artery where the adventitia is loading bearing, in the vagina, the adventitia is comprised of loose connective tissue that plays a primary role in attaching the vagina to the surrounding pelvic organs. Based on this it was hypothesized that collagen uncrimping within the subepithelium will dominate the creep response of the vaginal wall. Therefore, we evaluated collagen organization in the inner wall and not the outer wall (adventitia).

The open source CT-FIRE software (LOCI, Madison, WI²) quantified collagen fiber straightness ratio and fiber angle for each fiber [66]. A value of 1 for the straightness ratio denotes that the fiber is straight (i.e., not crimped/undulated). The open source CURVEALIGN software performed a bulk assessment of collagen features quantifying the alignment ratio. A value of 1 indicates perfectly aligned fibers, and smaller values represented more randomly distributed fibers [67]. Analysis was performed for each image.

2.8 Statistics. Statistical analysis was performed by hypothesis. A Shapiro–Wilk normality test evaluated the normal distribution of the data. A One-way ANOVA or nonparametric Kruskal–Wallis test evaluated the effect of pressure on Peleg's constants, initial creep rate, and creep strain at 100 s, with Tukey's or Dunn's posthoc test when necessary. A One-way ANOVA or nonparametric Kruskal–Wallis test evaluated the effect of axial length on Peleg's constants, initial creep rate, and creep strain at 100 s. Pearson's or Spearman's test correlated circumferential stress or axial stretch with creep strain and initial creep rate. To determine differences between genotypes unpaired *t*-test or nonparametric Mann–Whitney U test evaluated Peleg's constants, initial creep rate, and creep strain at 5, 7, 10, and 15 mmHg. To determine differences between genotypes unpaired *t*-test or nonparametric Mann–Whitney U test evaluated axial stretch and circumferential stress. A two-way ANOVA evaluated the effect of genotype and location on the straightness ratio, with Tukey's posthoc test when necessary. A nonparametric Friedman's test evaluated the effect of genotype and location on the alignment ratio. This study set the level for statistical significance at *p* ≤ 0.05. R Statistical Software performed statistical analyses and results are reported as mean ± standard error of the mean (SEM).

3 Results

3.1 Pressure and Axial Length—Dependent Creep. In the *Fbln5^{+/+}* vagina, 10 and 15 mmHg resulted in an upward shift in the creep strain versus time curves compared to 5 and 7 mmHg (Fig. 3(a)). Pressure significantly affected Peleg's constant *k*₂

(*p* = 0.02) and creep strain at 100 s (*p* = 0.03) in the *Fbln5^{+/+}* vagina (Table 1). Peleg's constant *k*₂ significantly increased at 10 (*p* = 0.04) and 15 (*p* = 0.03) mmHg compared to 5 mmHg. Creep strain at 100 s significantly increased (*p* = 0.04) at 15 compared to 5 mmHg. The pressure did not significantly affect Peleg's constant *k*₂ and creep strain at 100 s in the *Fbln5^{+/-}* vagina. The pressure did not significantly affect Peleg's constant *k*₁ and the initial creep rate in the *Fbln5^{+/+}* and *Fbln5^{+/-}* vaginas. In the *Fbln5^{+/+}* vagina, 4% above the physiologic axial length resulted in an upward shift in the creep strain versus time curve compared to 4% below the physiologic axial length (Fig. 4(a)). Axial length, however, did not significantly affect Peleg's constants, initial creep rate, and creep strain at 100 s in the *Fbln5^{+/+}* and *Fbln5^{+/-}* vaginas (Table 2). The linear regression described the creep response reasonably well for all pressure conditions and axial lengths. The mean *R*² values are reported in Table 1 for the pressure-dependent test and Table 2 for the axial length-dependent test. Representative fits for each loading condition in both genotypes are shown in Fig. 7 available in the Supplemental Materials on the ASME Digital Collection.

3.2 Circumferential Stress and Axial Stretch Versus Creep. A plot of the circumferential Cauchy stress versus creep strain at 100 s (Fig. 5(a)) and initial creep rate (Fig. 5(c)) further evaluated the effect of loading by pressure on creep. The Pearson's correlation identified no significant linear correlation between circumferential stress and creep strain at 100 s in the *Fbln5^{+/+}* (*r* = 0.29, *p* = 0.13) and *Fbln5^{+/-}* (*r* = 0.22, *p* = 0.27) vaginas. The Pearson's correlation identified no significant linear correlation between circumferential stress and initial creep rate in the *Fbln5^{+/+}* (*r* = 0.33, *p* = 0.09) and *Fbln5^{+/-}* (*r* = 0.37, *p* = 0.06) vaginas. A plot of axial stretches versus creep strains at 100 s (Fig. 5(b)) and initial creep rate (Fig. 5(d)) further evaluated the effect of loading by axial extension. The Pearson's correlation identified no significant linear correlation between axial stretch and creep strain at 100 s in the *Fbln5^{+/+}* (*r* = -0.11, *p* = 0.49) and *Fbln5^{+/-}* (*r* = 0.19, *p* = 0.27) vaginas. The Spearman's correlation identified no significant linear correlation between axial stretch and initial creep rate in the *Fbln5^{+/+}* (*ρ* = -0.06, *p* = 0.75) and *Fbln5^{+/-}* (*ρ* = 0.23, *p* = 0.18) vaginas.

3.3 Effect of Genotype on Creep. Due to pressure significantly affecting creep in the *Fbln5^{+/+}* vagina, creep was evaluated at each pressure (5, 7, 10, and 15 mmHg) to facilitate comparisons of creep behavior between genotypes. Unpaired *t*-test and Mann–Whitney *U* test did not detect significant differences between genotype at each pressure for Peleg's constants, initial creep rate, and creep strain at 100 s (See Table 2 available in the Supplemental Materials). This study evaluated if differences existed between genotype in circumferential stress calculated

²<http://www.loci.wisc.edu/software/curvealign>

from pressure-dependent creep ($n=7$ /genotype; See Table 3 available in the [Supplemental Materials](#) on the ASME Digital Collection). Unpaired t -test did not detect significant differences between genotype in circumferential stress due to applied pressures at 5, 7, 10, and 15 mmHg. Further, this study evaluated if differences existed between genotype in the axial stretch from axial length-dependent creep ($n=7$ /genotype; See Table 3 available in the [Supplemental Materials](#)). Unpaired t -test did not detect significant differences between genotype at axial stretches of 4% below, 2% below, physiologic, 2% above, and 4% above the physiologic length.

3.4 Microstructural Analysis. SHG imaging through the subepithelium from the epithelial side ($0\ \mu\text{m}$) toward the muscularis ($50\ \mu\text{m}$) permitted evaluating collagen organization and undulation (Figs. 6(a) and 6(b)). A two-way ANOVA for location and genotype demonstrated that location significantly affected ($p < 0.001$) the mean straightness ratio (Fig. 6(c)). Genotype did not significantly affect the mean straightness ratio and the statistical analysis did not detect significant interactions. Tukey's post-hoc test for location differences (independent of genotype) demonstrated that the straightness ratio significantly increased at 30 ($p = 0.01$), 40 ($p = 0.01$), and 50 ($p = 0.003$) μm , compared to $0\ \mu\text{m}$. A value of 1 for the straightness ratio denoted that the fiber was straight. At $0\ \mu\text{m}$ the axially oriented collagen fibers (80 deg to 90 deg and -80 deg to -90 deg) had an average straightness ratio of 0.87 in the *Fbln5*^{+/+} vagina (Fig. 7(a)) and 0.94 in the *Fbln5*^{+/-} (Fig. 7(b)). At $50\ \mu\text{m}$ the axially oriented collagen fibers had an average straightness ratio of 0.94 in the *Fbln5*^{+/+} and *Fbln5*^{+/-} vaginas. At $0\ \mu\text{m}$ the circumferentially oriented collagen fibers (-10 deg to 10 deg) had an average straightness ratio of 0.91 in the *Fbln5*^{+/+} and *Fbln5*^{+/-} vaginas. At $50\ \mu\text{m}$ the circumferentially oriented collagen fibers had an average straightness ratio of 0.91 in the *Fbln5*^{+/+} vagina and 0.93 in the *Fbln5*^{+/-}.

The nonparametric Friedman's test did not identify significant differences in location and genotype for the collagen alignment ratio (Fig. 6(d)). At $0\ \mu\text{m}$ 10% of the fibers were oriented axially (80 deg to 90 deg and -80 deg to -90 deg) in the *Fbln5*^{+/+} vagina (Fig. 7(c)) and 19% in the *Fbln5*^{+/-} (Fig. 7(d)). At $50\ \mu\text{m}$ 11% of the fibers were oriented axially in the *Fbln5*^{+/+} vagina and 25% in the *Fbln5*^{+/-}. At $0\ \mu\text{m}$ 8% of the fibers were oriented circumferentially (-10 deg to 10 deg) in the *Fbln5*^{+/+} vagina and 14% in the *Fbln5*^{+/-}. At $50\ \mu\text{m}$ 11% of the fibers were oriented circumferentially in the *Fbln5*^{+/+} vagina and 6% in the *Fbln5*^{+/-}.

4 Discussion

Creep describes the ability of a material to deform in response to a sustained constant load. In the vagina, creep may play a role in pelvic stability which is critical for maintaining the normal anatomy of the pelvic organs. In this study, we developed methods using extension-inflation testing to quantify vaginal creep under various circumferential and axial loads. Then, the protocol was applied to quantify vaginal creep and collagen microstructure in the fibulin-5 wildtype and haploinsufficient vaginas. The extension-inflation creep protocols and data analysis effectively evaluated the nonlinear circumferential vaginal creep response in the wildtype control and fibulin-5 haploinsufficient vaginas. This study demonstrated that circumferential loading by pressure significantly affected creep strain in the wildtype control vagina, but not the fibulin-5 haploinsufficient vagina. Further, that axial loading by extension did not significantly affect circumferential creep in the wildtype control and fibulin-5 haploinsufficient vaginas.

In the wildtype control vagina, an increase in pressure significantly increased creep strain. This corresponds with findings in the rabbit medial collateral ligament [26] and flexor tendon [60], where higher loads significantly increased creep strain compared to the lower loads. Although pressure affected the degree of deformation (creep strain), it did not significantly affect the rate of deformation (initial creep rate). The loads applied in this study

may have not been large enough to affect the initial rate of creep. In the rat skin, the rate of creep minimally changed under lower stress condition, however, under higher levels of stress the creep rate grew disproportionately faster [25]. This study evaluated creep within an estimated physiologically relevant pressure range. The pressure did not exceed three times the in vivo measured mean pressure, as in humans intravaginal pressure measurements change 2–3 folds with everyday activities from laying down (1.44 kPa; 11 mmHg) to sitting (3.66 kPa; 27 mmHg), walking (3.44 kPa; 26 mmHg), and running (4.39 kPa; 33 mmHg) [22]. These values are noted to be much higher during vaginal birth. In humans, the pressure between the vaginal wall and fetal head reaches up to 32 kPa (240 mmHg) with voluntary pushing [68]. This suggests that higher levels of pressure may permit further investigating the relationship between circumferential loading and creep rate.

Furthermore, this finding opposes the creep response in the rat cervix, where creep rate increased with circumferential loading from $4.7\ \text{min}^{-1}$ ($0.07\ \text{s}^{-1}$) under 20 grams to $14.9\ \text{min}^{-1}$ ($0.24\ \text{s}^{-1}$) under 60 grams [21]. Differences may be due to the rat cervix creep response being evaluated on day 22 of pregnancy, but herein, the murine vagina was nonpregnant. The vagina [38,69–71] and cervix [72–74] undergo significant microstructural remodeling by late pregnancy, with an increase in vaginal [4] and cervical [21,75,76] deformation during creep compared to the nonpregnant state. The significant increase in vaginal creep with pregnancy [4] suggests that loading may also affect creep rate in the pregnant vagina, however, future work is needed to confirm or refute this hypothesis. Quantification of the vaginal loading environment during physiological processes and disease may improve the evaluation of vaginal creep. Ultimately in this study, changes in creep strain with pressure but not initial creep rate demonstrated that the degree and rate of circumferential deformation did not directly correspond with each other, therefore, both metrics may be critical during future analysis.

The axial length did not statistically significantly affect creep strain at 100 s or the initial creep rate in both genotypes. In the murine vagina, an investigation of the elastic properties demonstrated that axial extension 4% above and 4% below the physiologic length did not significantly affect material stiffness along the circumferential direction [30]. During loading, the circumferential Cauchy stress versus circumferential stretch curve transitioned from the toe to linear region at 2.3 kPa for the 4% below test and 2.4 kPa for the 4% above test [30]. The axial Cauchy stress versus circumferential stretch curve transitioned at 1.4 kPa for the 4% below test and 6.2 kPa for the 4% above test [30]. This demonstrates that axial length may have a greater influence on the transition axial Cauchy stress, as it displayed minimal changes in the transition circumferential Cauchy stress between the two loading conditions. Hence, axial extension may not significantly affect circumferential Cauchy stress nor the circumferential creep response. Alternatively, the large variability in the axial length-dependent creep test may have influenced the statistical outcome. Two of the wildtype animals creep strains at 100 s ranged between 0.006 and 0.01 across all axial lengths, however, a Grubbs' test did not detect statistically significant outliers. Furthermore, the littermate haploinsufficient vaginas displayed a similar creep response suggesting that this may be a biological phenomenon versus an experimental outlier.

This study did not detect significant differences in creep between genotypes when comparing the creep response at the 5, 7, 10, and 15 mmHg. This was surprising because the wildtype vagina circumferential creep behavior depended on pressure and the haploinsufficient vagina was pressure independent. This suggests that the wildtype and haploinsufficient creep response were similar, however, that the wildtype vagina adapted to changes in intravaginal pressure. A creep study in the medial collateral ligament suggests that collagen fiber recruitment minimizes creep at low stress levels [26]. At higher levels of stress, a greater portion of collagen fibers was recruited and crimp/undulation decreased

during the elastic deformation, therefore, leaving fewer fibers to be recruited during creep [26]. This may result in a greater creep response under higher levels of stress as the load can no longer be shared over the load bearing area [26]. These previous findings suggest that the collagen fibers in the haploinsufficient vagina may be more undulated, thus as load increases it is able to minimize significant changes in creep strain through collagen fiber recruitment. This study, however, demonstrated no significant differences in collagen undulation between the haploinsufficient vagina and wildtype control in the subepithelium. Discrepancies may be a result of evaluating collagen undulation in the unloaded planar configuration and creep in the native intact tubular state. Due to limited depth penetration with SHG, imaging in the tubular configuration restricts imaging to the outer most layers, adventitia and muscularis [32].

This study aimed to evaluate collagen undulation and organization within the collagen dominated load-bearing subepithelial layer (inner layer) [71], thus requiring the tissue in a planar configuration. In the porcine coronary artery, collagen fibers showed a high degree of crimping in the native intact tube state with the collagen fibers uncrimping in the planar configuration [77]. It was initially hypothesized that the changes that occurred between the intact tubular state to the planar configuration would be similar among genotype thus making them comparable. The creep data, however, may imply that this may not hold true. Furthermore, a microscope limited to linear polarization imaged the collagen fibers. This may serve as a limitation because the fibers will display a stronger signal when oriented in the same direction as the incoming beam as opposed to rotated 90 deg to the beam. This may impact the orientation distribution and undulation analysis; however, it theoretically should have a greater impact on collagen fibers that are highly aligned such as in tendons and ligaments as opposed to fibers with a uniform random distribution. Despite this, limited information to date exists on collagen organization and undulation in the vagina [32,78,79], therefore, this study still provides necessary initial information to the field. Future work evaluating collagen fiber recruitment simultaneously during creep experiments will improve our understanding of the microstructural processes that contribute to the creep phenomenon in the vagina [26,80–82].

A second reason supporting why there were no significant differences between genotype in creep but differences in the pressure-dependent response may be due to collagen fiber interactions with the ground matrix. In the medial collateral ligament, an increase in water content significantly increases creep [83]. Further, tissues with higher water content had a significantly greater water loss. Thornton et al. study suggested that the amount and movement of water may allow greater interfibrillar movement. Herein, it is hypothesized that a lower water content may not allow as much fiber movement thus resulting in minimal differences in creep at higher pressures, as observed in the haploinsufficient vagina. Future work, however, is needed to investigate the effect of water content on creep in the vagina and if water content differs between the two genotypes to support or refute this hypothesis.

Evaluating vaginal creep relative to other pelvic structures and soft tissue may be critical for elucidating its role in pelvic support. Over the 100 s the vagina initially crept circumferentially on average $0.02\text{--}0.04\text{ s}^{-1}$. The swine and human uterosacral ligament, which plays a role in Level I support of the pelvic organs, crept on average $0.02\text{--}0.04\text{ s}^{-1}$ over 1200 s along with the main loading and perpendicular directions [84]. As for creep strain, herein 100 s of creep resulted in strain increasing between 0.002 and 0.01 (0.20–1.00%). In the human uterosacral ligament strain increased along the main loading direction from the average initial strain of 2.78% to near 3.00% resulting in a difference of 0.22% in creep strain [84]. These values are relatively lower than tissues outside of the pelvic cavity. In the rabbit flexor, tendons creep strain ranged between 2.00 and 4.00% [60]. While the values reported appear to be similar between the vagina and uterosacral

ligament but greater for the flexor tendon, interpretation and direct comparison across these structures, however, remains challenging. Various testing methods from uniaxial, planar biaxial, to biaxial extension-inflation investigated creep. A prior study demonstrated that testing methods significantly affected creep. In the amnion, a membrane that covers the fetal side of the placenta, creep significantly decreased using inflation testing compared to uniaxial tensile testing [85]. Standardization of protocols and loading conditions can improve cross comparison to evaluate differences in creep across the pelvic structures and changes that occur with pelvic floor disorders.

This study is not without limitations as it evaluated creep only along the circumferential direction. A previous study demonstrated greater stress relaxation along the axial direction compared to the circumferential direction in the gilt vagina [3]. This suggests that creep along the axial direction may also be important. The linear axial motor remained fixed through the duration of the creep test, thus limiting the ability to assess creep axially. An inflation device with a free axial extension would be an ideal setup to simultaneously evaluate creep circumferentially and axially. Such devices previously assessed vaginal tearing and rupture in the rat vagina [34]. Despite the system being fixed axially, this permitted assessing the effect of axial extension demonstrating that axial length 4% above and below the physiologic length did not significantly affect circumferential creep in the nonpregnant murine vagina. To the author's knowledge, this is the first study in the vagina evaluating the effect of circumferential and axial loading on creep. This study, therefore, provides initial information on vaginal creep to support the needs for future studies. Second, within this study, the passive viscoelastic properties were evaluated thus neglecting the active contribution from smooth muscle cells. Smooth muscle cells actively contribute to vaginal function circumferentially and axially [32,86], and smooth muscle tone significantly contributes to the elastic mechanical properties of the murine vagina [32]. In the colon, smooth muscle cells contribute to creep resulting in a significant increase in extension compared to the relaxed state [87,88]. Together these findings suggest that smooth muscle cells may contribute to viscoelastic creep in the vagina.

Further, all samples were frozen before mechanical testing. The freeze thaw cycle may induce microstructural changes resulting in different viscoelastic mechanical properties compared to testing freshly isolated tissue (See Fig. 8 available in the [Supplemental Materials](#) on the ASME Digital Collection). This study was designed based on prior studies in the female reproductive system so that findings can be compared to the published data. To date most viscoelastic studies in female reproductive tissue characterize the properties of previously frozen tissue [2,3,5,89–92]. Despite this limitation, all samples were prepared the same and presented a consistent and repeatable mechanical response. Further, independent of the preservation method the relationships observed within this study still should be observed on fresh tissue. This study still provided valuable methods to assess creep in the vagina under altered mechanical loading conditions that can be applied to other tubular organs. Additionally, the current study only evaluated collagen fibers. However, a concurrent study in fibulin-5 mice evaluated elastin area fraction and elastic fiber morphology demonstrating a decrease in elastin area fraction along the axial plane in the haploinsufficient mice compared to the wild-type [93]. Lastly, SHG imaging evaluated collagen microstructure in a planar configuration and not the intact tubular state as previously discussed. Future work characterizing freshly isolated vaginal tissue and accounting for smooth muscle cells contribution to creep is critical, as women with prolapse display a significant decrease in vaginal smooth muscle content [94–97]. Solely evaluating the passive components (e.g., collagen fibers), however, is a great initial step to elucidate how the passive matrix contributes to the creep phenomenon in the vagina as this unknown. After elucidating the passive microstructural processes that dictate vaginal creep, the active smooth muscle contribution is then needed.

5 Conclusion

The findings within this study suggest that the creep response to loading may vary with biological processes and pathologies, therefore, evaluating vaginal circumferential creep behavior under various circumferential loads may be important. Further, it highlighted the need for evaluating the degree and rate of deformation, as both metrics provide valuable information on vaginal creep behavior. The methods developed in this study may be useful for future work evaluating changes in vaginal creep throughout pregnancy, postpartum, and aging. Quantifying vaginal creep and elucidating the key microstructural processes that dictate vaginal creep is critical to understand why failures in pelvic organ support occur and how to improve current preventative and treatment strategies.

Acknowledgment

We acknowledge Dr. Hiromi Yanagisawa for developing the *Fbln5* mice and Dr. Jay D. Humphrey for providing the initial breeding pairs for the colony.

Funding Data

- Division of Civil, Mechanical and Manufacturing Innovation, NSF Faculty Early Career Development (Award no. 1751050 (K.S.M.); Funder ID: 10.13039/100000147).
- NSF (Award No. 1929731 (R.D.); Funder ID: 10.13039/100000001).

References

- [1] Fu, X., Siltberg, H., Johnson, P., and Ulmsten, U., 1995, "Viscoelastic Properties and Muscular Function of the Human Anterior Vaginal Wall," *Int. Urogynecol. J.*, **6**(4), pp. 229–234.
- [2] Feola, A., Duerr, R., Moalli, P., and Abramowitch, S., 2013, "Changes in the Rheological Behavior of the Vagina in Women With Pelvic Organ Prolapse," *Int. Urogynecol. J.*, **24**(7), pp. 1221–1227.
- [3] Pack, E., Dubik, J., Snyder, W., Simon, A., Clark, S., and De Vita, R., 2020, "Biaxial Stress Relaxation of Vaginal Tissue in Pubertal Girls," *ASME J. Biomech. Eng.*, **142**(3), p. 031002.
- [4] Weli, H. K., Akhtar, R., Chang, Z., Li, W. W., Cooper, J., and Yang, Y., 2017, "Advanced Glycation Products' Levels and Mechanical Properties of Vaginal Tissue in Pregnancy," *Eur. J. Obstetrics Gynecol. Reproductive Biol.*, **214**, pp. 78–85.
- [5] Pena, E., Calvo, B., Martinez, M. A., Martins, P., Mascarenhas, T., Jorge, R. M. N., Ferreira, A., and Doblare, M., 2010, "Experimental Study and Constitutive Modeling of the Viscoelastic Mechanical Properties of the Human Prolapsed Vaginal Tissue," *Biomech. Model. Mechanobiol.*, **9**(1), pp. 35–44.
- [6] Epstein, L. B., Graham, C. A., and Heit, M. H., 2008, "Impact of Sacral Colpopexy on In Vivo Vaginal Biomechanical Properties," *Am. J. Obstet. Gynecol.*, **199**(6), pp. 664.e1–664.e6.
- [7] Rubod, C., Boukerrou, M., Briue, M., Dubois, P., and Cosson, M., 2007, "Biomechanical Properties of Vaginal Tissue. Part 1: New Experimental Protocol," *J. Urol.*, **178**(1), pp. 320–325.
- [8] Epstein, L. B., Graham, C. A., and Heit, M. H., 2007, "Systemic and Vaginal Biomechanical Properties of Women With Normal Vaginal Support and Pelvic Organ Prolapse," *Am. J. Obstet. Gynecol.*, **197**(2), pp. 165.e1–165.e6.
- [9] Chuong, C. J., Ma, M., Eberhart, R. C., and Zimmern, P., 2014, "Viscoelastic Properties Measurement of the Prolapsed Anterior Vaginal Wall: A Patient-Directed Methodology," *Eur. J. Obstet. Gynecol. Reprod. Biol.*, **173**, pp. 106–112.
- [10] Wu, J. M., Matthews, C. A., Conover, M. M., Pate, V., and Funk, M. J., 2014, "Lifetime Risk of Stress Urinary Incontinence or Pelvic Organ Prolapse Surgery," *Obstet. Gynecol.*, **123**(6), pp. 1201–1206.
- [11] Olsen, A. L., Smith, V. J., Bergstrom, J. O., Colling, J. C., and Clark, A. L., 1997, "Epidemiology of Surgically Managed Pelvic Organ Prolapse and Urinary Incontinence," *Obstet. Gynecol.*, **89**(4), pp. 501–506.
- [12] Mant, J., Painter, R., and Vessey, M., 1997, "Epidemiology of Genital Prolapse: Observations From the Oxford Family Planning Association Study," *Brit. J. Obstet. Gynaecol.*, **104**(5), pp. 579–585.
- [13] Noblett, K. L., Jensen, J. K., and Ostergard, D. R., 1997, "The Relationship of Body Mass Index to Intra-Abdominal Pressure as Measured by Multichannel Cystometry," *Int. Urogynecol. J. Pelvic Floor Dysfunct.*, **8**(6), pp. 323–326.
- [14] Vergeldt, T. F. M., Weemhoff, M., IntHout, J., and Kluivers, K. B., 2015, "Risk Factors for Pelvic Organ Prolapse and Its Recurrence: A Systematic Review," *Int. Urogynecol. J.*, **26**(11), pp. 1559–1573.
- [15] Jorgensen, S., Hein, H. O., and Gyntelberg, F., 1994, "Heavy Lifting at Work and Risk of Genital Prolapse and Herniated Lumbar Disc in Assistant Nurses," *Occup. Med.-Oxford*, **44**(1), pp. 47–49.
- [16] Pouca, M., Ferreira, J. P. S., Oliveira, D. A., Parente, M. P. L., and Jorge, R. M. N., 2018, "Viscous Effects in Pelvic Floor Muscles During Childbirth: A Numerical Study," *Int. J. Numer. Methods Biomed. Eng.*, **34**(3), p. e2927.
- [17] Ashton-Miller, J. A., and DeLancey, J. O. L., 2009, "On the Biomechanics of Vaginal Birth and Common Sequelae," *Ann. Rev. Biomed. Eng.*, **11**, pp. 163–176.
- [18] Lien, K. C., DeLancey, J. O. L., and Ashton-Miller, J. A., 2009, "Biomechanical Analyses of the Efficacy of Patterns of Maternal Effort on Second-Stage Progress," *Obstet. Gynecol.*, **113**(4), pp. 873–880.
- [19] Tracy, P. V., Wadhvani, S., Triebwasser, J., Wineman, A. S., Orejuela, F. J., Ramin, S. M., DeLancey, J. O., and Ashton-Miller, J. A., 2018, "On the Variation in Maternal Birth Canal In Vivo Viscoelastic Properties and Their Effect on the Predicted Length of Active Second Stage and Levator Ani Tears," *J. Biomech.*, **74**, pp. 64–71.
- [20] Clark, K., Ji, H. L., Feltovich, H., Janowski, J., Carroll, C., and Chien, E. K., 2006, "Mifepristone-Induced Cervical Ripening: Structural, Biomechanical, and Molecular Events," *Am. J. Obstet. Gynecol.*, **194**(5), pp. 1391–1398.
- [21] Williams, L. M., Hollingsworth, M., and Dixon, J. S., 1982, "Changes in the Tensile Properties and Fine-Structure of the Rat Cervix in Late Pregnancy and During Parturition," *J. Reprod. Fertil.*, **66**(1), pp. 203–211.&
- [22] Kruger, J., Hayward, L., Nielsen, P., Loiselle, D., and Kirton, R., 2013, "Design and Development of a Novel Intra-Vaginal Pressure Sensor," *Int. Urogynecol. J.*, **24**(10), pp. 1715–1721.
- [23] Shaw, J. M., Hamad, N. M., Coleman, T. J., Egger, M. J., Hsu, Y., Hitchcock, R., and Nygaard, I. E., 2014, "Intra-Abdominal Pressures During Activity in Women Using an Intra-Vaginal Pressure Transducer," *J. Sports Sci.*, **32**(12), pp. 1176–1185.
- [24] Dietze-Hermosa, M., Hitchcock, R., Nygaard, I. E., and Shaw, J. M., 2020, "Intra-Abdominal Pressure and Pelvic Floor Health: Should We Be Thinking About This Relationship Differently?," *Female Pelvic Med. Reconstr. Surg.*, **26**(7), pp. 409–414.
- [25] Chen, G., Cui, S. B., You, L., Li, Y., Mei, Y. H., and Chen, X., 2015, "Experimental Study on Multi-Step Creep Properties of Rat Skins," *J. Mech. Behav. Biomed. Mater.*, **46**, pp. 49–58.
- [26] Thornton, G. M., Shrive, N. G., and Frank, C. B., 2002, "Ligament Creep Recruits Fibres at Low Stresses and Can Lead to Modulus-Reducing Fibre Damage at Higher Creep Stresses: A Study in Rabbit Medial Collateral Ligament Model," *J. Orthop. Res.*, **20**(5), pp. 967–974.
- [27] Skalak, T. C., and Schmid-Schönbein, G. W., 1986, "Viscoelastic Properties of Microvessels in Rat Spinotrapezius Muscle," *ASME J. Biomech. Eng.*, **108**(3), pp. 193–200.
- [28] Carniel, E. L., Mencattelli, M., Bonsignori, G., Fontanella, C. G., Frigo, A., Rubini, A., Stefanini, C., and Natali, A. N., 2015, "Analysis of the Structural Behaviour of Colonic Segments by Inflation Tests: Experimental Activity and Physio-Mechanical Model," *Proc. Inst. Mech. Eng. Part H-J. Eng. Med.*, **229**(11), pp. 794–803.
- [29] Weizsacker, H. W., Lambert, H., and Pascale, K., 1983, "Analysis of the Passive Mechanical-Properties of Rat Carotid Arteries," *J. Biomech.*, **16**(9), pp. 703–715.
- [30] Robison, K. M., Conway, C. K., Desrosiers, L., Knoepp, L. R., and Miller, K. S., 2017, "Biaxial Mechanical Assessment of the Murine Vaginal Wall Using Extension-Inflation Testing," *ASME J. Biomech. Eng.*, **139**(10), p. 104504.
- [31] Akintunde, A., Robison, K. M., Capone, D., Desrosiers, L., Knoepp, L. R., and Miller, K. S., 2018, "Effects of Elastase Digestion on the Murine Vaginal Wall Biaxial Mechanical Response," *ASME J. Biomech. Eng.*, **141**(2), p. 021011.
- [32] Clark, G. L., Pokutta-Paskaleva, A. P., Lawrence, D. J., Lindsey, S. H., Desrosiers, L., Knoepp, L. R., Bayer, C. L., Gleason, R. L., and Miller, K. S., 2019, "Smooth Muscle Regional Contribution to Vaginal Wall Function," *Interface Focus*, **9**(4), p. 20190025.
- [33] White, S. E., Conway, C. K., Clark, G. L., Lawrence, D. J., Bayer, C. L., and Miller, K. S., 2019, "Biaxial Basal Tone and Passive Testing of the Murine Reproductive System Using a Pressure Myograph," *Jove-J. Visualized Exp.*, (150), p. 13.
- [34] McGuire, J. A., Crandall, C. L., Abramowitch, S. D., and De Vita, R., 2019, "Inflation and Rupture of Vaginal Tissue," *Interface Focus*, **9**(4), p. 20190029.
- [35] Ali, A. F., Taha, M. M. R., Thornton, G. M., Shrive, N. G., and Frank, C. B., 2005, "Biomechanical Study Using Fuzzy Systems to Quantify Collagen Fiber Recruitment and Predict Creep of the Rabbit Medial Collateral Ligament," *ASME J. Biomech. Eng.*, **127**(3), pp. 484–493.
- [36] Ferruzzi, J., Collins, M. J., Yeh, A. T., and Humphrey, J. D., 2011, "Mechanical Assessment of Elastin Integrity in Fibrillin-1-Deficient Carotid Arteries: Implications for Marfan Syndrome," *Cardiovasc. Res.*, **92**(2), pp. 287–295.
- [37] Ferruzzi, J., Bersi, M. R., Mecham, R. P., Ramirez, F., Yanagisawa, H., Tellides, G., and Humphrey, J. D., 2016, "Loss of Elastic Fiber Integrity Compromises Common Carotid Artery Function: Implications for Vascular Aging," *Artery Res.*, **14**(C), pp. 41–52.
- [38] Drewes, P. G., Yanagisawa, H., Starcher, B., Hornstra, I., Csiszar, K., Marinis, S. I., Keller, P., and Word, R. A., 2007, "Pelvic Organ Prolapse in Fibrillin-5 Knockout Mice—Pregnancy-Induced Changes in Elastic Fiber Homeostasis in Mouse Vagina," *Am. J. Pathol.*, **170**(2), pp. 578–589.
- [39] Wieslander, C. K., Rahn, D. D., McIntire, D. D., Acevedo, J. F., Drewes, P. G., Yanagisawa, H., and Word, R. A., 2009, "Quantification of Pelvic Organ Prolapse in Mice: Vaginal Protease Activity Precedes Increased MOPQ Scores in Fibulin 5 Knockout Mice," *Biol. Reprod.*, **80**(3), pp. 407–414.

- [40] Lau, A. C., Duong, T. T., Ito, S., and Yeung, R. S. M., 2008, "Matrix Metalloproteinase 9 Activity Leads to Elastin Breakdown in an Animal Model of Kawasaki Disease," *Arthritis Rheum.*, **58**(3), pp. 854–863.
- [41] Budatha, M., Roshanravan, S., Zheng, Q., Weislander, C., Chapman, S. L., Davis, E. C., Starcher, B., Word, R. A., and Yanagisawa, H., 2011, "Extracellular Matrix Proteases Contribute to Progression of Pelvic Organ Prolapse in Mice and Humans," *J. Clin. Invest.*, **121**(5), pp. 2048–2059.
- [42] Yanagisawa, H., Davis, E. C., Starcher, B. C., Ouchi, T., Yanagisawa, M., Richardson, J. A., and Olson, E. N., 2002, "Fibulin-5 is an Elastin-Binding Protein Essential for Elastic Fibre Development In Vivo," *Nature*, **415**(6868), pp. 168–171.
- [43] Byers, S. L., Wiles, M. V., Dunn, S. L., and Taft, R. A., 2012, "Mouse Estrous Cycle Identification Tool and Images," *PLoS One*, **7**(4), p. e35538.
- [44] Kevin, F., Joanne, C., and DE, H., 2007, *The Mouse in Biomedical Research*, Elsevier, Burlington, MA.
- [45] Danso, E. K., Schuster, J. D., Johnson, I., Harville, E. W., Buckner, L. R., Desrosiers, L., Knoepf, L. R., and Miller, K. S., 2020, "Comparison of Biaxial Biomechanical Properties of Post-Menopausal Human Prolapsed and Non-Prolapsed Uterosacral Ligament," *Sci. Rep.*, **10**(1), p. 14.
- [46] van der Walt, I., Bo, K., Hanekom, S., and Rienhardt, G., 2014, "Ethnic Differences in Pelvic Floor Muscle Strength and Endurance in South African Women," *Int. Urogynecol. J.*, **25**(6), pp. 799–805.
- [47] Park, K., Goldstein, I., Andry, C., Siroky, M. B., Krane, R. J., and Azadzi, K. M., 1997, "Vasculogenic Female Sexual Dysfunction: The Hemodynamic Basis for Vaginal Engorgement Insufficiency and Clitoral Erectile Insufficiency," *Int. J. Impotence Res.*, **9**(1), pp. 27–37.
- [48] Nagabukuro, H., and Berkley, K. J., 2007, "Influence of Endometriosis on Visceromotor and Cardiovascular Responses Induced by Vaginal Distention in the Rat," *Pain*, **132**(Suppl. 1), pp. S96–S103.
- [49] Cason, A. M., Samuelsen, C. L., and Berkley, K. J., 2003, "Estrous Changes in Vaginal Nociception in a Rat Model of Endometriosis," *Hormones Behav.*, **44**(2), pp. 123–131.
- [50] Wang, Z. J., Lakes, R. S., Golob, M., Eickhoff, J. C., and Chesler, N. C., 2013, "Changes in Large Pulmonary Arterial Viscoelasticity in Chronic Pulmonary Hypertension," *PLoS One*, **8**(11), p. e78569.
- [51] Ferruzzi, J., Bersi, M. R., and Humphrey, J. D., 2013, "Biomechanical Phenotyping of Central Arteries in Health and Disease: Advantages of and Methods for Murine Models," *Ann. Biomed. Eng.*, **41**(7), pp. 1311–1330.
- [52] Amin, M., Le, V. P., and Wagenseil, J. E., 2012, "Mechanical Testing of Mouse Carotid Arteries: From Newborn to Adult," *Jove-J. Visual. Exp.*, (60), p. 9.
- [53] van Loon, P., Klip, W., and Bradley, E. L., 1977, "Length-Force and Volume-Pressure Relationships of Arteries," *Biorheology*, **14**(4), pp. 181–201.
- [54] Manley, E., Provenzano, P. P., Heisey, D., Lakes, R., and Vanderby, R., 2003, "Required Test Duration for Group Comparisons in Ligament Viscoelasticity: A Statistical Approach," *Biorheology*, **40**(4), pp. 441–450.
- [55] Provenzano, P., Lakes, R., Keenan, T., and Vanderby, R., 2001, "Nonlinear Ligament Viscoelasticity," *Ann. Biomed. Eng.*, **29**(10), pp. 908–914.
- [56] Turner, S., 1973, "Creep in Glassy Polymers," *The Physics of Glassy Polymers*, Wiley, New York.
- [57] Hingorani, R. V., Provenzano, P. P., Lakes, R. S., Escarcega, A., and Vanderby, R., 2004, "Nonlinear Viscoelasticity in Rabbit Medial Collateral Ligament," *Ann. Biomed. Eng.*, **32**(2), pp. 306–312.
- [58] Panayi, D. C., Digesu, G. A., Tekkis, P., Fernando, R., and Khullar, V., 2010, "Ultrasound Measurement of Vaginal Wall Thickness: A Novel and Reliable Technique," *Int. Urogynecol. J.*, **21**(10), pp. 1265–1270.
- [59] Humphrey, J. D., 2002, *Cardiovascular Solid Mechanics: Cells, Tissues, and Organs*, Springer, New York.
- [60] Asundi, K. R., and Rempel, D. M., 2008, "MMP-1, IL-1 Beta, and COX-2 mRNA Expression is Modulated by Static Load in Rabbit Flexor Tendons," *Ann. Biomed. Eng.*, **36**(2), pp. 237–243.
- [61] Thornton, G. M., Boorman, R. S., Shrive, N. G., and Frank, C. B., 2002, "Medial Collateral Ligament Autografts Have Increased Creep Response for at Least Two Years and Early Immobilization Makes This Worse," *J. Orthop. Res.*, **20**(2), pp. 346–352.
- [62] Thornton, G. M., Leask, G. P., Shrive, N. G., and Frank, C. B., 2000, "Early Medial Collateral Ligament Scars Have Inferior Creep Behaviour," *J. Orthop. Res.*, **18**(2), pp. 238–246.
- [63] Peleg, M., 1979, "A Model for Creep and Early Failure," *Mater. Sci. Eng.*, **40**(2), pp. 197–205.
- [64] Solomon, W. K., and Jindal, V. K., 2017, "Application of Peleg's Equation to Describe Creep Responses of Potatoes Under Constant and Variable Storage Conditions," *J. Texture Stud.*, **48**(3), pp. 193–197.
- [65] Peleg, M., 1979, "Characterization of the Stress Relaxation Curves of Solid Foods," *J. Food Sci.*, **44**(1), pp. 277–281.
- [66] Bredfeldt, J. S., Liu, Y. M., Pehlke, C. A., Conklin, M. W., Szulczewski, J. M., Inman, D. R., Keely, P. J., Nowak, R. D., Mackie, T. R., and Eliceiri, K. W., 2014, "Computational Segmentation of Collagen Fibers From Second-Harmonic Generation Images of Breast Cancer," *J. Biomed. Opt.*, **19**(1), p. 016007.
- [67] Bredfeldt, J. S., Liu, Y., Conklin, M. W., Keely, P. J., Mackie, T. R., and Eliceiri, K. W., 2014, "Automated Quantification of Aligned Collagen for Human Breast Carcinoma Prognosis," *J. Pathol. Inform.*, **5**(1), p. 28.
- [68] Rempen, A., and Kraus, M., 1991, "Pressures on the Fetal Head During Normal Labor," *J. Perinatal Med.*, **19**(3), pp. 199–206.
- [69] Downing, K. T., Billah, M., Raparia, E., Shah, A., Silverstein, M. C., Ahmad, A., and Boutis, G. S., 2014, "The Role of Mode of Delivery on Elastic Fiber Architecture and Vaginal Vault Elasticity: A Rodent Model Study," *J. Mech. Behav. Biomed. Mater.*, **29**, pp. 190–198.
- [70] Ulrich, D., Edwards, S. L., Su, K., White, J. F., Ramshaw, J. A. M., Jenkin, G., Deprest, J., Rosamilia, A., Werkmeister, J. A., and Gargett, C. E., 2014, "Influence of Reproductive Status on Tissue Composition and Biomechanical Properties of Ovine Vagina," *PLoS One*, **9**(4), p. e93172.
- [71] Rynkevicius, R., Martins, P., Hympanova, L., Almeida, H., Fernandes, A. A., and Deprest, J., 2017, "Biomechanical and Morphological Properties of the Multiparous Ovine Vagina and Effect of Subsequent Pregnancy," *J. Biomech.*, **57**, pp. 94–102.
- [72] Nallasamy, S., Yoshida, K., Akins, M., Myers, K., Iozzo, R., and Mahendroo, M., 2017, "Steroid Hormones Are Key Modulators of Tissue Mechanical Function Via Regulation of Collagen and Elastic Fibers," *Endocrinology*, **158**(4), pp. 950–962.
- [73] Yoshida, K., Jiang, H. F., Kim, M., Vink, J., Cremers, S., Paik, D., Wapner, R., Mahendroo, M., and Myers, K., 2014, "Quantitative Evaluation of Collagen Crosslinks and Corresponding Tensile Mechanical Properties in Mouse Cervical Tissue During Normal Pregnancy," *PLoS One*, **9**(11), p. e112391.
- [74] Myers, K., Socrate, S., Tzeranis, D., and House, M., 2009, "Changes in the Biochemical Constituents and Morphologic Appearance of the Human Cervical Stroma During Pregnancy," *Eur. J. Obstet. Gynecol. Reprod. Biol.*, **144**, pp. S82–S89.
- [75] Kokenyesi, R., Armstrong, L. C., Agah, A., Artal, R., and Bornstein, P., 2004, "Thrombospondin 2 Deficiency in Pregnant Mice Results in Premature Softening of the Uterine Cervix," *Biol. Reprod.*, **70**(2), pp. 385–390.
- [76] Kokenyesi, R., and Woessner, J. F., 1990, "Relationship Between Dilatation of the Rat Uterine Cervix and a Small Dermatan Sulfate Proteoglycan," *Biol. Reprod.*, **42**(1), pp. 87–97.
- [77] Keyes, J. T., Lockwood, D. R., Utzinger, U., Montilla, L. G., Witte, R. S., and Vande Geest, J. P., 2013, "Comparisons of Planar and Tubular Biaxial Tensile Testing Protocols of the Same Porcine Coronary Arteries," *Ann. Biomed. Eng.*, **41**(7), pp. 1579–1591.
- [78] Sikora, M., Scheiner, D., Betschart, C., Perucchini, D., Mateos, J. M., di Natale, A., Fink, D., and Maake, C., 2015, "Label-Free, Three-Dimensional Multiphoton Microscopy of the Connective Tissue in the Anterior Vaginal Wall," *Int. Urogynecol. J.*, **26**(5), pp. 685–691.
- [79] McGuire, J. A., Monclova, J. L., Coariti, A. C. S., Stine, C. A., Toussaint, K. C., Munson, J. M., Dillard, D. A., and De Vita, R., 2021, "Tear Propagation in Vaginal Tissue Under Inflation," *Acta Biomater.*, **127**, pp. 193–204.
- [80] Miller, K. S., Connizzo, B. K., Feeney, E., and Soslowsky, L. J., 2012, "Characterizing Local Collagen Fiber Re-Alignment and Crimp Behavior Throughout Mechanical Testing in a Mature Mouse Supraspinatus Tendon Model," *J. Biomech.*, **45**(12), pp. 2061–2065.
- [81] Miller, K. S., Connizzo, B. K., Feeney, E., Tucker, J. J., and Soslowsky, L. J., 2012, "Examining Differences in Local Collagen Fiber Crimp Frequency Throughout Mechanical Testing in a Developmental Mouse Supraspinatus Tendon Model," *ASME J. Biomech. Eng.*, **134**(4), p. 041004.
- [82] Chow, M. J., Turcotte, R., Lin, C. P., and Zhang, Y. H., 2014, "Arterial Extracellular Matrix: A Mechanobiological Study of the Contributions and Interactions of Elastin and Collagen," *Biophys. J.*, **106**(12), pp. 2684–2692.
- [83] Thornton, G. M., Shrive, N. G., and Frank, C. B., 2001, "Altering Ligament Water Content Affects Ligament Pre-Stress and Creep Behaviour," *J. Orthop. Res.*, **19**(5), pp. 845–851.
- [84] Baah-Dwomoh, A., Alperin, M., Cook, M., and De Vita, R., 2018, "Mechanical Analysis of the Uterosacral Ligament: Swine vs. Human," *Ann. Biomed. Eng.*, **46**(12), pp. 2036–2047.
- [85] Mauri, A., Perrini, M., Ehret, A. E., De Focatiis, D. S., and Mazza, E., 2015, "Time-Dependent Mechanical Behavior of Human Amnion: Macroscopic and Microscopic Characterization," *Acta Biomater.*, **11**, pp. 314–323.
- [86] Huntington, A., Rizzuto, E., Abramowitch, S., Del Prete, Z., and De Vita, R., 2019, "Anisotropy of the Passive and Active Rat Vagina Under Biaxial Loading," *Ann. Biomed. Eng.*, **47**(1), pp. 272–281.
- [87] Greven, K., Rudolph, K. H., and Hohorst, B., 1976, "Creep After Loading in the Relaxed and Contracted Smooth Muscle (Taenia Coli of the Guinea Pig) Under Various Osmotic Conditions," *Pflugers Arch.*, **362**(3), pp. 255–260.
- [88] Hohorst, B., Krohnert, U., and Greven, K., 1976, "Passive Stress Relaxation Followed by Active Contraction in Vertebrate Smooth Muscles (Taenia Coli of the Guinea Pig)," *Pflugers Arch.*, **366**(2–3), pp. 137–142.
- [89] Chien, E. K., Ji, H. L., Feltoovich, H., and Clark, K., 2005, "Expression of Matrix Metalloproteinase-3 in the Rat Cervix During Pregnancy and in Response to Prostaglandin E-2," *Am. J. Obstet. Gynecol.*, **192**(1), pp. 309–317.
- [90] Barone, W. R., Feola, A. J., Moalli, P. A., and Abramowitch, S. D., 2012, "The Effect of Pregnancy and Postpartum Recovery on the Viscoelastic Behavior of the Rat Cervix," *J. Mech. Med. Biol.*, **12**(01), p. 1250009.
- [91] Feltoovich, H., Ji, H. L., Janowski, J. W., Delancey, N. C., Moran, C. C., and Chien, E. K., 2005, "Effects of Selective and Nonselective PGE2 Receptor Agonists on Cervical Tensile Strength, and Collagen Organization and Microstructure in the Pregnant Rat at Term," *Am. J. Obstet. Gynecol.*, **192**(3), pp. 753–760.
- [92] Poellmann, M. J., Chien, E. K., McFarlin, B. L., and Johnson, A. J. W., 2013, "Mechanical and Structural Changes of the Rat Cervix in Late-Stage Pregnancy," *J. Mech. Behav. Biomed. Mater.*, **17**, pp. 66–75.
- [93] Clark-Patterson, G. L. R., Sambit, D., Laurephile, K., Sen, L., and Aritro Sen Miller, K. S., "Role of Fibulin-5 Insufficiency and Prolapse Progression on Murine Vaginal Biomechanical Function," *Sci. Rep.*, epub.

- [94] Boreham, M. K., Wai, C. Y., Miller, R. T., Schaffer, J. I., and Word, R. A., 2002, "Morphometric Properties of the Posterior Vaginal Wall in Women With Pelvic Organ Prolapse," *Am. J. Obstet. Gynecol.*, **187**(6), pp. 1501–1508.
- [95] Boreham, M. K., Wai, C. Y., Miller, R. T., Schaffer, J. I., and Word, R. A., 2002, "Morphometric Analysis of Smooth Muscle in the Anterior Vaginal Wall of Women With Pelvic Organ Prolapse," *Am. J. Obstet. Gynecol.*, **187**(1), pp. 56–63.
- [96] Badiou, W., Granier, G., Bousquet, P. J., Monrozier, X., Mares, P., and de Tayrac, R., 2008, "Comparative Histological Analysis of Anterior Vaginal Wall in Women With Pelvic Organ Prolapse or Control Subjects. A Pilot Study," *Int. Urogynecol. J.*, **19**(5), pp. 723–729.
- [97] Takacs, P., Gualtieri, M., Nassiri, M., Candiotti, K., and Medina, C. A., 2008, "Vaginal Smooth Muscle Cell Apoptosis is Increased in Women With Pelvic Organ Prolapse," *Int. Urogynecol. J.*, **19**(11), pp. 1559–1564.